

Nuclear relaxation in a randomly diluted Heisenberg paramagnet

Pradeep Thayamballi and Daniel Hone

Physics Department, University of California, Santa Barbara, California 93106

(Received 16 July 1979)

The high (room)-temperature relaxation rates of those ^{19}F nuclei which are not transfer hyperfine coupled to Mn spins in $\text{KMn}_x\text{Mg}_{1-x}\text{F}_3$ are calculated as a function of Mn concentration. Good agreement with experiment is found for the theoretical results, which have been obtained in the concentration range $0.02 \leq x < 1$ (excluding values near the critical percolation concentration $x_c = 0.31$). The time dependence of the nuclear-spin decay is found to be well represented by $\exp[-(t/\tau)^n]$, with n varying smoothly from $n=1$ at $x=1$ to $n \approx 0.5$ for $x \ll 1$. The second-neighbor exchange constant between Mn spins needed for agreement with experiment is found to be smaller than an independently, but also indirectly, measured value.

I. INTRODUCTION

Among the simplest and most studied of the insulating antiferromagnets is KMnF_3 , a cubic perovskite crystal with a Heisenberg superexchange between nearest-neighbor Mn spins on the simple cubic lattice sites, mediated by an F ion at the midpoint of each cube edge. Thus each fluorine has two manganese nearest neighbors, with each of which the ^{19}F nucleus interacts strongly by an isotropic transferred hyperfine coupling $A\bar{I} \cdot (\bar{S}_1 + \bar{S}_2)$. Above the Néel temperature the resonance frequency of a ^{19}F nucleus is therefore shifted by an amount proportional to $A(\langle S_{1z} \rangle + \langle S_{2z} \rangle)$, where z is the direction of the applied static field. In a magnetically diluted crystal, $\text{KMn}_x\text{Mg}_{1-x}\text{F}_3$, where a fraction $(1-x)$ of the manganese ions have been replaced by nonmagnetic magnesium ions, there is essentially no distortion of the lattice and at room temperature three distinct ^{19}F nuclear resonance lines are observed,¹ corresponding to fluorines missing two, one, or zero manganese nearest neighbors and their accompanying hyperfine fields. Borsa and Jaccarino,¹ who studied the relaxation at room temperature of the ^{19}F nuclei with no Mn nearest neighbors observed a remarkably sharp rise in the relaxation rates as the Mn concentration x was decreased from unity. This rise implies a strong increase in the low-frequency fluctuations of the dipolar fields of the Mn spins, an effect which they attributed to the increasing [with $(1-x)$] number of Mn spins which are exchange isolated from their (nearest) neighbors (see Fig. 1). These exchange-isolated spins then decay only via the relatively weak electronic dipolar interactions which remain—i.e., their fluctuation power spectrum extends only to dipolar, rather than to exchange frequencies, and there is much more spectral weight at the low frequencies required to relax the ^{19}F nuclei.

Here we explore this notion in detail. We calculate the relaxation of ^{19}F nuclear spins in $\text{KMn}_x\text{Mg}_{1-x}\text{F}_3$ for manganese concentrations $0.01 < x < 1$. The experiments do not extend below this range, and, in addition, at lower concentrations nuclear-spin diffusion starts to play an important role, requiring a different theoretical treatment.² Furthermore, we have not been able to treat values of x very close to the critical percolation concentration ($x_c = 0.31$ for a simple cubic lattice), but experiment does not suggest any dramatic behavior in the nuclear relaxation in that region. The experimental results have been reported in terms of simple exponential decay rates. Although the theory developed here predicts more complicated

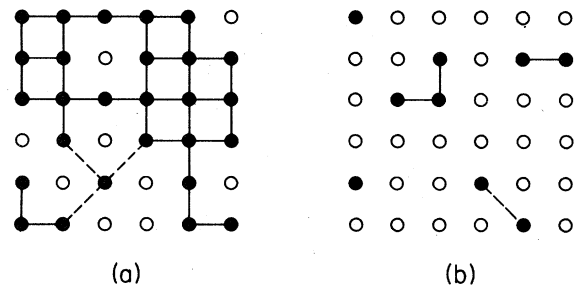


FIG. 1. Two-dimensional representation of types of configurations and interactions arising (a) above and (b) below the percolation limit. The solid lines denote nearest-neighbor exchange interactions between Mn spins (solid circles) and the dashed lines second-neighbor exchange interactions. Open circles represent nonmagnetic Mg atoms. All spins, of course, are dipolar coupled. We show part of the infinite cluster, as well as an "isolated" spin in part (a), and in part (b) four isolated spins, a two- and a three-spin cluster.

time dependence for the relaxation, appropriate exponential fits to the theory give results in good agreement with experiment. However, the theory also suggests that a more careful experimental study would give interesting new results.

In Sec. II we discuss the general theory. Sections III and IV are devoted to concentrations substantially above and well below the critical percolation concentration x_c , respectively, and the numerical results and conclusions, including comparison with experiment, are given in Sec. V.

$$\frac{1}{T_1(\bar{r}_n)} = \frac{1}{2} (\gamma_e \gamma_n \hbar)^2 \sum_j r_{jn}^{-6} \left\{ F_j(\alpha\beta\gamma; \alpha_j\beta_j\gamma_j) \int_{-\infty}^{\infty} dt \cos\omega_0 t \langle S_j^z(t) S_j^z(0) \rangle \right. \\ \left. + \frac{1}{2} F_j'(\alpha\beta\gamma; \alpha_j\beta_j\gamma_j) \int_{-\infty}^{\infty} dt \cos\omega_0 t [\langle S_j^+(t) S_j^-(0) \rangle + \langle S_j^-(t) S_j^+(0) \rangle] \right\}, \quad (2.1)$$

where the sum is over sites occupied by Mn spins, at distances r_{jn} from the nucleus in question; $\omega_0 = \gamma_n H_0$ is the nuclear Zeeman frequency; α, β, γ are the direction cosines of the external field with respect to the crystal axes; and $\alpha_j, \beta_j, \gamma_j$ are the corresponding direction cosines of the vectors \bar{r}_{jn} connecting nuclear and electron-spin sites. The coefficients F_j and F_j' depend only on the direction cosines indicated; they are the usual angular parts of the squares of dipole interaction matrix elements. Because the experiments were done on powder samples, we will average over field direction (relative to the local crystalline axes), and these coefficients simply become

$$F_j = \frac{2}{3} + 2\gamma_j^2, \quad F_j' = \frac{4}{3} + 2(1 - \gamma_j^2). \quad (2.2)$$

The expression (2.1) neglects all terms involving the correlations of two different Mn spins. In pure KMnF_3 the pair correlations between the two Mn spins equally hyperfine coupled to a ^{19}F nucleus contribute about 20%⁴ to the nuclear resonance linewidth or to the nuclear relaxation, at high temperatures. In the present problem, exchange-coupled pairs contribute appreciably to the relaxation only very near $x = 1.0$, where we may be making, at most, a 20% error by excluding them. Moreover, exchange-isolated spins, which will turn out to dominate the relaxation process in most cases, are much more weakly (dipole) coupled to other spins, and pair correlations are correspondingly much smaller; we neglect their contribution. We discuss the effect briefly when we consider the influence of small exchange-coupled clusters (particularly pairs), exchange isolated from the remaining Mn spins, in Sec. IV.

The electron-spin dynamics appear formally in the relaxation calculation [Eq. (2.1)] in the evaluation of two-spin autocorrelation functions $\langle S_j^\alpha(t) S_j^\beta(0) \rangle$, where the time dependence of the operators is

II. GENERAL THEORY

The ^{19}F nuclear spins being studied have only non-magnetic nearest neighbors, and therefore they interact with the Mn spins only through nuclear-electron dipolar forces. The corresponding relaxation times are far longer than the correlation times of all Mn spins, even those which are isolated. Thus any given ^{19}F spin, at a position \bar{r}_n , will relax exponentially, with a rate $1/T_1(\bar{r}_n)$ given approximately³ by first-order time-dependent perturbation theory:

governed by the Hamiltonian

$$\mathcal{H}_e = \gamma_e \mathcal{H}_0 \sum_i S_i^z + \sum_{i>j} J_{ij} \bar{S}_i \cdot \bar{S}_j \\ + \gamma_e^2 \sum_{i>j} [\bar{S}_i \cdot \bar{S}_j - 3(\bar{S}_i \cdot \hat{r}_{ij})(\bar{S}_j \cdot \hat{r}_{ij})] r_{ij}^{-6}, \quad (2.3)$$

where the sums are over sites occupied by Mn ions, and the three terms on the right-hand side represent the Zeeman, exchange, and dipolar interactions. Although there is a very weak exchange between second-nearest neighbors, as discussed below, the nearest-neighbor exchange strength is overwhelmingly dominant, and when we speak of "exchange-coupled" spins below we refer to nearest neighbors only, unless explicitly indicated otherwise.

The experiments with which we want to compare this theory were carried out at room temperature, far above the (concentration-dependent) ordering temperature ($T_N = 88$ K at $x = 1$). We therefore calculate the electronic autocorrelation functions at infinite temperature

$$\langle AB \rangle = \text{Tr}(AB) / \text{Tr}(1). \quad (2.4)$$

Even in this limit we cannot, in general, calculate these functions exactly. However, we require only their Fourier transforms at the nuclear Zeeman frequency ω_0 . Since electronic correlation times, of the order of exchange or dipolar times, are orders of magnitude smaller than ω_0^{-1} , we can in fact take the zero-frequency transform. We follow the standard procedure⁵ of approximating the correlation function by exponential extrapolation of its leading short-time behavior

$$\langle S_j^\alpha(t) S_j^\beta(0) \rangle \approx 1 - \gamma t^n \approx \exp(-\gamma t^n). \quad (2.5)$$

In the disordered system we must sum over all Mn

environments of the nuclei and over all environments of each Mn spin in calculating its autocorrelation function. Within the approximation (2.5) the needed low-frequency Fourier transform of the autocorrelation function is proportional to $\gamma^{-(1/n)}$. Rather than attempting a configuration average of this, however, we will simply average γ itself.

With configuration averaging the decay of the total nuclear magnetization will be a weighted sum of simple exponentials, resulting in general in nonexponential decay

$$\langle I^z(t) I^z(0) \rangle \propto \prod_j \left[1 - \sum_k p_k [1 - \exp(-\alpha_{jk} t)] \right], \quad (2.6)$$

where k classifies the type of Mn spin according to its dynamics (isolated spin, member of an exchange-coupled pair, member of the infinite exchange-coupled cluster, etc.) and p_k is the probability of a spin of type k occupying the site j (so that $\sum p_k = x$). The rate α_{jk} is the contribution to $1/T_1$ in Eq. (2.1) from a spin of type k at the site j . It contains the

$$\langle I^z(t) I^z(0) \rangle / \langle (I^z)^2 \rangle \approx \exp \left\{ -\frac{4}{3} \pi N_0 x [\rho^3 (e^{-\alpha t / \rho^6} - 1) + (\alpha \pi t)^{1/2} \text{erf}(\alpha t / \rho^6)] \right\}, \quad (2.8)$$

where N_0 is the number of lattice sites per unit volume, and ρ is the smallest distance in the sum over sites j (or the lower limit on the corresponding integral). At times for which $\alpha t / \rho^6 \gg 1$, Eq. (2.8) predicts a decay of the form $\exp[-(t/\tau)^{1/2}]$, a result discussed and observed experimentally by McHenry *et al.*⁶ We expect it to be applicable for low concentrations, $x \ll x_c$.

III. HIGH CONCENTRATIONS: $x > x_c$

Above the percolation limit, $x > x_c$, the nuclei interact both with spins of the infinite cluster and with finite exchange-isolated clusters. The corresponding relaxation rates α_{jk} [see Eq. (2.6)] are determined [Eq. (2.3)] by the spin autocorrelation functions on site j , $\langle S_j^\alpha(t) S_j^\beta(0) \rangle$. Here the time dependence of the operators is governed by the electronic Hamiltonian H_e of Eq. (2.3).

If S_j is a member of the infinite cluster, then the dipolar and Zeeman interactions in H_e can be neglected in the calculation of the autocorrelation functions. In this approximation, and in the cubic lattice and at the high temperatures of interest here, those autocorrelation functions are isotropic in spin space:

$$\langle S_j^\alpha(t) S_j^\beta(0) \rangle \approx \delta_{\alpha\beta} \langle S_j^z(t) S_j^z(0) \rangle, \quad (3.1)$$

for the infinite cluster, at least after averaging over the environment of the site j (while maintaining it in the infinite cluster). We can further usefully make

factor $\gamma^{(-1/n)}$, discussed above, appropriate to an electron spin of type k , and the coupling constant, angular factors, and r_j^{-6} from the electron-nuclear dipole interaction. In the spirit of the assumption of randomness of the alloy, we neglect any correlations between the occupancies of different sites. All of this, of course, presumes as adequate the approximation that the local environment of a spin (in particular, the size of the cluster of which it is a member) determines its dynamics and its consequent contribution to the nuclear relaxation.

If k is limited to a single value, then $p_k = x$ and Eq. (2.6) has two simple limits. If $x \rightarrow 1$ then Eq. (2.6) becomes a simple exponential. If $x \ll 1$, then that equation can be approximated by

$$\langle I^z(t) I^z(0) \rangle \approx \exp \left[-x \sum_j [1 - \exp(-\alpha_j t)] \right]. \quad (2.7)$$

Furthermore, if we can ignore the angular factors in α_j , so that $\alpha_j \approx \alpha r_j^{-6}$, and if the sum over sites is approximated by a spatial integral, then

the standard approximation of a Gaussian decay of the autocorrelation function, with a rate determined by the second time derivative at $t=0$:

$$\langle S_j^z(t) S_j^z(0) \rangle \approx \left[\frac{1}{3} S(S+1) \right] \exp \left(-\frac{1}{2} \omega_{ej}^2 t^2 \right), \quad (3.2)$$

where the "exchange frequency" at site j is

$$\omega_{ej}^2 = \left[\frac{2}{3} S(S+1) \sum J_{jl}^2 \right] \approx \frac{2}{3} S(S+1) z_j J^2. \quad (3.3)$$

In the final equality we have neglected all beyond nearest-neighbor exchange constants, and z_j is the number of magnetic nearest neighbors to the spin at j in the particular configuration considered. We require the Fourier transform of Eq. (3.2) at the nuclear Zeeman frequency $\omega_0 \ll \omega_{ej}$ for the nuclear relaxation rate:

$$\int_{-\infty}^{\infty} \cos \omega_0 t \langle S_j^z(t) S_j^z(0) \rangle \approx \frac{S(S+1)}{3} \frac{\sqrt{2\pi}}{\omega_{ej}}. \quad (3.4)$$

In the sum over nuclei we will encounter all possible environments of an infinite-cluster spin at the relative position j ; the proper configuration average is therefore $\langle 1/\omega_e \rangle$. However, at least away from the percolation limit $x = x_c$, we do not seriously err in replacing this by $1/\langle \omega_e \rangle \propto x^{-1/2}$ [note the similar approximation made following Eq. (2.5)]. Here we have averaged the coordination number $\langle z \rangle = 6x$, as if averaging over all spins, rather than just those in the infinite cluster, but these averages are virtually identical over the range of x near $x=1$ where this infinite-cluster contribution is significant. If we take seriously the expression (3.3) for ω_e , then in pure

KMnF₃, using the value $J/k = 7.60 \pm 0.08$ K from inelastic neutron scattering results,⁷ we find $\omega_e(x=1) \approx 5.9 \times 10^{12} \text{ sec}^{-1}$. If, on the other hand, we interpret ω_e as a measure of the low-frequency spectral weight of spin fluctuations, through Eq. (3.4), then the NMR linewidth of ¹⁹F in the pure material⁸ implies $\omega_e \approx 3.6 \times 10^{12} \text{ sec}^{-1}$. The difference in these values has its origin, of course, in the assumption (3.2) of a pure Gaussian decay of the spin autocorrelation function which neglects, for example, the long-time diffusive behavior.⁹ The latter interpretation is clearly more physically relevant to the nuclear relaxation problem, and we therefore use the smaller value of ω_e in the numerical calculations below. Again, with the exception of values of x very close to x_c , we have for the probability p_∞ that any site j is occupied by a member of the infinite cluster, $p_\infty \approx x$. Then the infinite cluster contribution to the relaxation of the ¹⁹F nuclei is approximately an exponential decay:

$$\exp(-\gamma_\infty t); \quad \gamma_\infty(x) = 990\sqrt{x} \text{ sec}^{-1}. \quad (3.5)$$

$$\langle S_j^\alpha(t) S_j^\beta(0) \rangle = K_{\alpha\beta} \frac{1}{3} S(S+1) \exp \left[- \int_0^t d\tau (t-\tau) \frac{\langle [\tilde{\mathcal{H}}'(\tau) \cdot \tilde{S}_j(\tau)] [S_j^\beta \mathcal{H}'] \rangle}{\langle S_j^\alpha S_j^\beta \rangle} \right], \quad (3.6)$$

where

$$K_{zz} = 1, \quad K_{+-} = K_{-+}^* = 2 \exp(\pm i\omega_z t), \quad (3.7)$$

and all other $K_{\alpha\beta} = 0$; ω_z is the electronic Zeeman frequency. The interaction picture operators $\tilde{\mathcal{H}}'(\tau)$ and $\tilde{S}_j(\tau)$ in the exponent have a time dependence generated by the Zeeman and nearest-neighbor exchange Hamiltonians above. The commutators in the exponent give four-spin correlation functions of the form $\langle S_i^\alpha(\tau) S_j^\beta(\tau) S_l^\gamma S_l^\rho \rangle$, where i and l are explicitly not equal to j . In this high-concentration range ($x > 0.45$) fewer than 3% of the spins are isolated, so it is highly unlikely for the isolated spin S_j to find another isolated spin in its first few neighboring shells. Therefore, S_j is almost certainly relaxed dominantly by spins S_i and S_l (in the above four-spin correlation function) which are in the infinite cluster. Then this correlation function decays in a time of order ω_e^{-1} , the exchange time, and the isolated spin operator $\tilde{S}_j^\alpha(\tau) = S_j \exp(i\alpha\omega_z\tau)$ can be replaced by S_j^α . Further, S_j is only weakly coupled to S_i and S_l , and for the dominant term ($i=l$) the four-spin function can be approximately factored

$$\langle S_i^\alpha(\tau) S_j^\beta(\tau) S_l^\gamma S_l^\rho \rangle \approx \delta_{il} \langle S_i^\alpha(\tau) S_l^\rho \rangle \langle S_j^\beta S_j^\gamma \rangle. \quad (3.8)$$

The times t of interest in Eq. (3.6) are much longer than exchange times, so the upper limit on the in-

We note that this computed result appears to agree well with the $x \rightarrow 1$ limit of the experimental values reported in Ref. 1. We have computed this contribution somewhat crudely, not only in the configuration averaging procedure already discussed, but also in ignoring the topological structure of the cluster, which may develop¹⁰ substantial numbers of linear strings (locally one dimensional) or plates (locally two dimensional) and quite different long-time diffusional behavior¹¹ than at $x=1$. This would alter the dependence of the effective ω_e [see Eq. (3.4)] on concentration x . But we will see that this infinite-cluster contribution is of importance only very near $x=1$, where the approximations made are certainly adequate.

We turn now to the contribution to the nuclear relaxation from the isolated spins (with no exchange-coupled nearest neighbors). To calculate their autocorrelation functions, we treat the dipolar and second-neighbor exchange parts of \mathcal{H}_e as a perturbation \mathcal{H}' within the interaction picture. A standard lowest-order cumulant expansion⁵ then gives

tegral can be replaced by ∞ and

$$\langle S_j^\alpha(t) S_j^\beta(0) \rangle \approx \frac{1}{3} S(S+1) \times \exp \left[-t\omega_e^{-1} \sum_i (a_{1i} J_2^2 + a_{2i} D_i^2) \right], \quad (3.9)$$

where the sum is over those sites i which are occupied by Mn ions. Here J_2 is the second-neighbor exchange strength and $a_{1i} \neq 0$ only if i and j are second neighbors. The constants a_{1i} and a_{2i} are of order $S(S+1)$, and D_i measures the dipole strength between spins at i and j . Since both J_2 and D are small compared to ω_e , these isolated spins decay much more slowly than those of the infinite cluster. Their low-frequency spectral power is of order $\omega_e^2/(J_2^2 + D^2) \geq 10^3$ times as large as that of spins in the infinite cluster, so they tend to dominate the nuclear relaxation, although they are few in number, up to values of $x \sim 0.7$. We have only considered longitudinal fluctuations (of the z component of \tilde{S}_j alone). From Eq. (3.6) we see that the spectral distribution of transverse fluctuations is centered about the electronic Zeeman frequency ω_z , with a width of order $(D^2 + J_2^2)/\omega_e \ll \omega_z$. Thus there is little spectral weight at the low frequencies required for nuclear re-

laxation, and the transverse fluctuations are ineffective in this process. This is, of course, a familiar effect in other contexts; for isolated spins there is no exchange narrowing.

In this numerical estimate of the relative efficiency of isolated spins, we required a value of J_2 . An analysis⁷ of inelastic neutron scattering data in pure KMnF_3 suggests a second-neighbor exchange there of order $J_2 \sim 0.03J$. But direct studies¹² of pairs of Mn spins in small concentrations in KMgF_3 suggest a much smaller value, $J_2 \approx (0.01 \pm 0.006)J$, when the intervening nearest-neighbor Mn ions are replaced by nonmagnetic Mg ions. This smaller value, clearly more appropriate to the present problem, is still several times larger than the dipolar interaction between second neighbors. In fact, we will discover below that even this value of J_2 appears to be somewhat too large.

IV. LOW CONCENTRATIONS: $x < x_c$

Below $x = x_c$ all clusters are finite, with a distribution in size which is increasingly dominated by the single isolated spins as x is reduced. We can conveniently treat only very small (and very large) clusters, so we limit consideration to $x < 0.1$, where the fractions of spins which are isolated, members of isolated pairs, or members of three-spin clusters are approximately 0.53, 0.21, and 0.10, respectively. As noted in the Introduction, we also do not consider $x < 0.01$, where nuclear-spin diffusion begins to play a role (since the nuclear dipole-dipole interaction becomes comparable to the nuclear level separation associated with different local environments).

We consider first the dynamics of the isolated spins, determined by the dipolar interactions with other nearby spins. If those other spins belong to large clusters then—just as with the infinite cluster discussed above—their effects are reduced by the rapid fluctuations due to the internal exchange interactions in the cluster. In fact, as we have just pointed out, in this concentration range it is most likely that the nearby Mn spins will themselves be isolated. If so, they relax the reference spin in a time characteristic of the dipolar interaction between the two:

$$\langle S_i^z(t) S_i^z(0) \rangle \approx \exp\left[-\sum_j D_{ij}^2 t^2\right],$$

where the sum is over the sites j of the isolated spins relaxing S_i , and D_{ij} contains the dipolar coupling constants, angular factors, and r_{ij}^{-6} . Because of the rapid r_{ij}^{-6} falloff in the exponent, we can classify the dynamics of S_i according to the distance at which the nearest Mn neighbor is found, with all relaxers beyond the unoccupied shells accounted for only within a configurational average. As in Sec. III, only the z component (longitudinal) fluctuation of the

exchange-isolated spin are effective in nuclear relaxation.

The total spin $\vec{S} = \vec{S}_1 + \vec{S}_2$ of an exchange-isolated Mn pair commutes with the exchange Hamiltonian; the decay of \vec{S} is governed by dipolar interactions, both internal and external to the pair. The effectiveness of the internal dipolar interactions is sharply reduced by the exchange-induced rapid fluctuations of the spins, while that of the external interactions is not; the latter fields become the major source of relaxation

$$\langle S^z(t) S^z(0) \rangle = \sum_{i,j=1}^2 \langle S_i^z(t) S_j^z(0) \rangle. \quad (4.1)$$

In this isolated cluster the strong exchange coupling relative to external interactions leads to pair correlations ($i \neq j$) as important as autocorrelations ($i = j$). If the spins 1 and 2 have identical external interactions, then

$$\langle S_i^z(t) S_i^z(0) \rangle = A(t), \quad \langle S_1^z(t) S_2^z(0) \rangle = P(t), \quad (4.2)$$

with $A(0) = \frac{1}{3}S(S+1)$ and $P(0) = 0$. We have $A(t) + P(t) \approx \text{constant}$ until times long enough for the dipolar interactions to be important. As spin information is communicated rapidly between the two spins, after a characteristic exchange time, τ_e , $A(t)$ and $P(t)$ each tends to an average value of $\frac{1}{6}S(S+1)$. Then both correlation functions (or their values averaged over several exchange times) decay in much the same way, as determined by the external interactions:

$$\bar{A}(t) = \bar{P}(t) \approx \left[\frac{1}{6}S(S+1)\right] \exp\left(-\frac{1}{2}w^2 t^2\right) \quad (t \gg \tau_e), \quad (4.3)$$

where w is a dipolar relaxation rate.

Let us consider the effect of an isolated pair on the relaxation of a nucleus whose distances from the two spins are r_1 and r_2 . The relevant terms contributing to the relaxation rate are

$$A(t)(r_1^{-6} + r_2^{-6}) + 2P(t)r_1^{-3}r_2^{-3}. \quad (4.4)$$

Thus, if $r_1 \approx r_2$, the pair acts effectively like two isolated spins at that distance. We make this approximation throughout our numerical calculations; we do not expect this to introduce appreciable error.

The description of exchange-isolated clusters of three or more spins can be made along the same lines, but the approximations clearly become worse as the cluster size increases. Thus, to the extent that internal dipole interactions can be neglected, the total z component of spin [initial average square value $\frac{1}{3}nS(S+1)$ for an n -spin cluster] decays in a time characteristic of its external dipolar interactions. Such a cluster relaxes nuclei at distances large com-

pared to cluster dimensions at a rate comparable to n isolated spins at the same distance. Of course, the contribution to the relaxation beyond a few lattice spacings from the nucleus becomes negligible, so the picture is of little utility for clusters larger than two or three spins. We must again, therefore, not deal with concentrations too close to the percolation limit x_c , where larger clusters begin to play an important role.

V. RESULTS AND DISCUSSION

The calculations described in the preceding sections were carried out numerically for a nucleus in the central cell of a cubic lattice 15 lattice spacings on a side. The full angular and distance dependence of the dipolar interactions was included, and configuration averages were made as discussed in Sec. II [see, in particular, Eq. (2.6)]. The results for the decay of the net nuclear magnetization, as a function of time, are shown for representative concentrations both above and below the percolation limit in Fig. 2. The (positive) curvature in all cases reflects the departure of the decay law from pure exponential behavior, with stronger departures for decreasing Mn concentrations x .

The curves were calculated with next-nearest-neighbor exchange J_2 set equal to zero. The justification for neglecting J_2 , in spite of earlier estimates^{7,12} placing its value greater than the dipole interaction between the same two spins, can be found in Fig. 3, where we have plotted the calculated ^{19}F nuclear relaxation appropriate to $x=0.5$ for $(J_2/J)=0.01$,

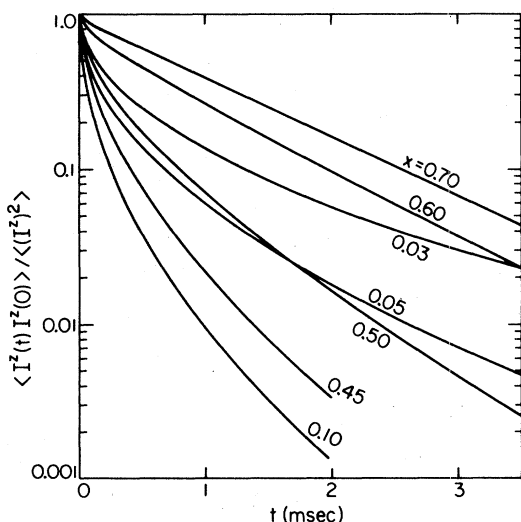


FIG. 2. Calculated decay of the nuclear magnetization as a function of time, with second-neighbor exchange $J_2=0$. Curves are labeled by Mn concentration x .

0.004, and zero, and compared these curves to experiment.¹ The first two values of (J_2/J) were chosen to represent Windsor's independent determination of this quantity¹² by resonance on Mn pairs, as 0.01 ± 0.006 . The form of the nuclear decay is seen to be quite sensitive to the value of J_2 in this range, and although the experimental curve¹³ has been arbitrarily normalized at $t=0.1$ msec, comparison with theory decidedly favors a value of (J_2/J) appreciably smaller than 0.004. The remarkable agreement with the $J_2=0$ theory is surely partly fortuitous, considering both the approximations which have been made in the theory and the experimental uncertainties ($\sim \pm 0.1x$) in the concentration x . Nevertheless, the comparison certainly suggests a value of (J_2/J) smaller than the lower limit of Ref. 12. We note that in the isostructural compound RbMnF_3 , with nearly identical transferred hyperfine interactions,¹⁴ a value of J only about 10% smaller, and a lattice parameter only 1% larger than that of KMnF_3 , the second-neighbor exchange J_2 is zero within experimental error.¹⁴

The experimental results of Ref. 1 were reported as values of $1/T_1$, characteristic of pure exponential decay, $\exp(-t/T_1)$. In fact, what is given there is the initial observed slope of the logarithm of the decay, after an experimental dead time of about 50 μsec . For comparison with those results, then, we have plotted the corresponding slopes of the theoretical curves in Fig. 4, along with the experimental values of Ref. 1. The agreement is good throughout the full concentration range where we have results. We note that, although there are no experimental results for $\text{KMn}_x\text{Mg}_{1-x}\text{F}_3$ below $x=0.1$, there are reported in

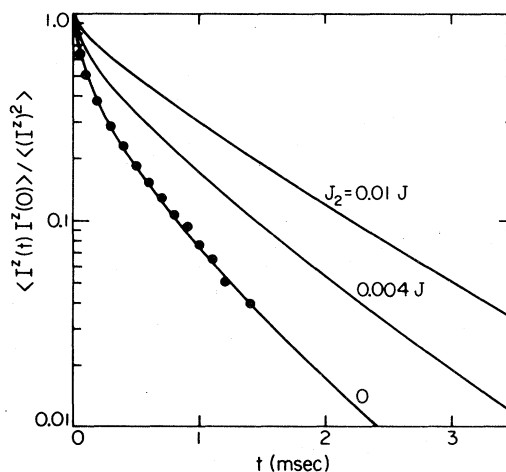


FIG. 3. Calculated decay of the nuclear magnetization for three values of J_2 , at fixed Mn concentration $x=0.5$. The circles are the experimental points, arbitrarily normalized at $t=0.1$ msec.

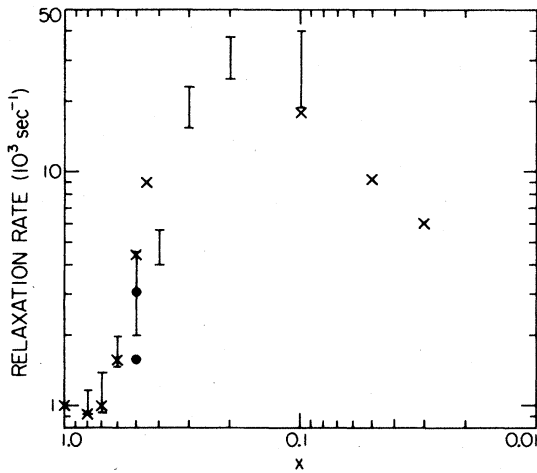


FIG. 4. Relaxation rate, defined as the logarithmic derivative of the nuclear decay at time $t = 50 \mu\text{sec}$, as a function of Mn concentration x . Theoretical values (see Fig. 2) are indicated by crosses, experimental values (from Ref. 1) by error bars. The circles at $x = 0.5$ are results for $J_2 = 0.01J$ (lower circle) and $J_2 = 0.004J$ (upper circle); all crosses are for $J_2 = 0$.

Ref. 1 some results for $\text{Mn}_x\text{Zn}_{1-x}\text{F}_2$ down to $x = 0.01$, and it is suggested there that the results for the two systems will be comparable. The value reported for $1/T_1$ at $x = 0.01$ is $0.5 \pm 0.3 (\text{msec})^{-1}$, which appears roughly consistent with an extrapolation of our theoretical predictions.

However, the curves in Fig. 2 clearly are not well characterized by their initial slopes alone. In view of the limiting cases of the decay at large times discussed in Sec. II [viz., $\exp(-t/\tau)$ as $x \rightarrow 1$ and $\exp(-\sqrt{t}/\sqrt{\tau})$ for $x \ll 1$], it seems reasonable to look for long-time behavior, for general x , of the form

$$f(t) \equiv \frac{\langle I^2(t)I^2(0) \rangle}{\langle (I^2)^2 \rangle} \sim A \exp[-(t/\tau)^n] \quad (5.1)$$

Then at times sufficiently long that $|\ln A| \ll (t/\tau)^n$, a log-log plot of $-\ln f(t)$ vs t should exhibit linear behavior, with slope n . Such behavior is indeed seen in Fig. 5, and the values of n and τ so determined are plotted in Fig. 6. We see the expected limiting values of $n = 1$ as $x \rightarrow 1$ and $n = 0.5$ for $x \ll 1$. The passage from one to the other occurs largely above the percolation limit $x > x_c = 0.31$. The dashed section of the curve represents a smooth interpolation in the region near x_c where we were unable to make adequate theoretical approximations. The relevant rate, $1/\tau$, appears to peak in this region. Clearly, it would be interesting to extend the experimental observations to compare in detail with the theoretical prediction and to explore the region near $x = x_c$.

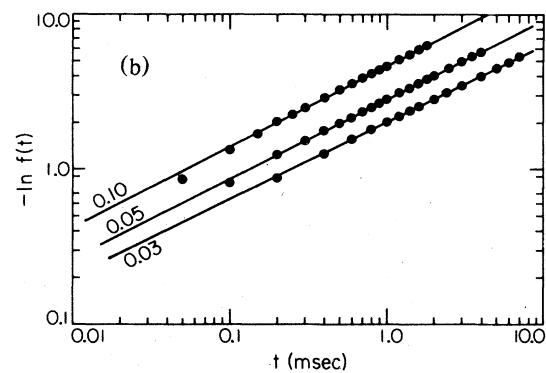
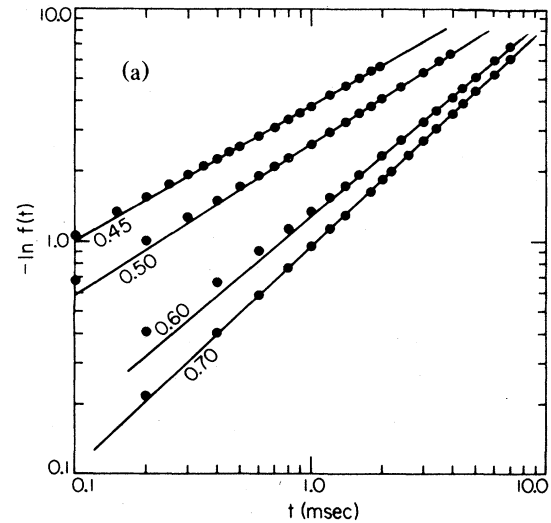


FIG. 5. The logarithm of the nuclear decay rate, as a function of time, plotted so as to exhibit directly the behavior (5.1). (a) concentrations $x > x_c$; (b) $x < x_c$. The curves are labeled by values of x .

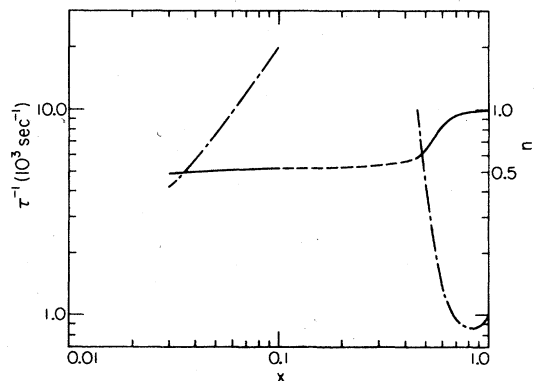


FIG. 6. Exponent n (solid line with dashed interpolation) and effective rate τ^{-1} (dot-dashed curve) characterizing nuclear decay in the form of Eq. (5.1).

ACKNOWLEDGMENTS

We are indebted to Dr. V. Jaccarino and Dr. F. Borsa for discussions of their experimental work¹ and interpretations of it, and for supplying us with some of the original data. We are grateful to Mario Bosco for helpful discussions of some early preliminary calculations he carried out on this problem. This work was supported in part by the NSF Grant No. DMR78-05926.

¹F. Borsa and V. Jaccarino, *Solid State Commun.* **19**, 1229 (1976).

²H. E. Rorschach, Jr., *Physica (Utrecht)* **30**, 38 (1964).

³T. Moriya, *Prog. Theor. Phys.* **16**, 23 (1956).

⁴D. W. Hone and B. G. Silbernagel, *J. Phys. (Paris)* **32**, C1-761 (1971).

⁵R. Kubo and K. Tomita, *J. Phys. Soc. Jpn.* **9**, 888 (1954).

⁶M. R. McHenry, B. G. Silbernagel, and J. H. Wernick, *Phys. Rev. B* **5**, 2958 (1972).

⁷S. J. Pickart, M. F. Collins, and C. G. Windsor, *J. Appl. Phys.* **37**, 1054 (1966).

⁸R. G. Shulman and K. Knox, *Phys. Rev.* **119**, 94 (1960).

⁹J. E. Gulley, D. W. Hone, D. J. Scalapino, and B. G. Silbernagel, *Phys. Rev. B* **1**, 1020 (1970).

¹⁰Near the percolation limit in two dimensions such effects

are observed in computer-generated random networks: H. E. Stanley, R. J. Birgeneau, P. J. Reynolds, and J. F. Nicoll, *J. Phys. C* **9**, L553 (1976). See also R. J. Birgeneau, R. A. Cowley, A. Shirane, and H. J. Guggenheim, *Phys. Rev. Lett.* **37**, 940 (1976).

¹¹R. E. Dietz *et al.*, *Phys. Rev. Lett.* **26**, 1186 (1971); P. M. Richards and M. B. Salamon, *Phys. Rev. B* **9**, 32 (1974).

¹²C. G. Windsor, Ph.D. thesis, Oxford, 1963 (unpublished), referred to in M. B. Walker, *Proc. Phys. Soc. London* **87**, 45 (1966), and in Ref. 7.

¹³Original experimental data kindly supplied by the authors of Ref. 1.

¹⁴M. B. Walker and R. W. H. Stevenson, *Proc. Phys. Soc. London* **87**, 35 (1966).